

## Nitrogen and sulfur conversion during pressurized pyrolysis under CO<sub>2</sub> atmosphere in fluidized bed

Yuanqiang Duan<sup>a</sup>, Lunbo Duan<sup>a, b, \*</sup>, Edward John Anthony<sup>b</sup>, Changsui Zhao<sup>a</sup>

\* Corresponding author: [duanlunbo@seu.edu.cn](mailto:duanlunbo@seu.edu.cn)

<sup>a</sup> Key Laboratory of Energy Thermal Conversion and Control, Ministry of Education, School of Energy and Environment, Southeast University, Nanjing 210096, China

<sup>b</sup> Centre for Combustion and CCS, Cranfield University, Cranfield, Bedfordshire MK43 0AL, UK

**Abstract:** Pressurized oxy-fuel combustion (POFC) is a promising technology for CO<sub>2</sub> capture from coal-fired power plants, offering both high efficiency and a low penalty. However, the high partial pressure of CO<sub>2</sub> in a POFC furnace has important impacts on fuel-N and fuel-S conversion during the coal pyrolysis process, and understanding this will help to achieve further control of SO<sub>x</sub>/NO<sub>x</sub>. In this study, coal pyrolysis experiments were conducted in a pressurized fluidized bed with the pressure range of 0.1–0.7 MPa under N<sub>2</sub> and CO<sub>2</sub> atmosphere. The gaseous products were monitored by a Fourier transform infrared spectroscopy analyzer (FTIR) and the char residue was characterized by an X-ray photoelectron spectroscopy (XPS) analyzer in order to acquire the species information for S-containing and N-containing compounds. Results show that the enrichment of CO<sub>2</sub> in the local atmosphere enhances the fuel-N conversion to HCN in the pyrolysis process, which serves as a favorable precursor to N<sub>2</sub>O. The generation of HCN and NH<sub>3</sub> increase simultaneously with the increase of overall pressure. SO<sub>2</sub> concentration in the gaseous product is relatively low, and as the pressure increases, the concentration decreases slightly due to CO reduction of SO<sub>2</sub> to COS. Sulfur content in the char decreases as the pressure goes from 0.1 MPa to 0.7 MPa indicating higher CO<sub>2</sub> pressure accelerates the decomposition of sulfur compounds in the coal, which is further confirmed by the XPS results.

**Key words:** pressurized oxy-fuel combustion; pyrolysis; CO<sub>2</sub> atmosphere; nitrogen conversion; sulfur speciation;

## 29 1. Introduction

30 Carbon capture and storage (CCS) technologies capture up to 90% of CO<sub>2</sub> emissions from a  
31 power plant or industrial facility and store them in underground geologic formations. The  
32 International Energy Agency (IEA) estimates that CCS can achieve 13% of the global greenhouse  
33 gas emissions reductions needed by 2050 to limit global warming to 2°C [1]. Carbon capture has  
34 been established for some industrial processes, but it is still a relatively expensive technology.  
35 Much effort needs to be devoted to reducing the cost of CCS technologies in the near future.

36 Oxy-fuel technology, as one of the major coal-fired power plant CCS technologies, has  
37 received much attention recently. In oxy-fuel technology, the process typically entails burning the  
38 fuel in a mixture of recycled flue gas and O<sub>2</sub> instead of air as the primary oxidant. The high CO<sub>2</sub>  
39 concentration in the flue gas makes it conducive to CO<sub>2</sub> separation. Also, other gaseous pollutants  
40 such as NO<sub>x</sub> and SO<sub>x</sub> can be simultaneously removed [2]. The biggest obstacle to the development  
41 and application of oxy-fuel technology at present is the net efficiency penalty associated with the  
42 high cost of the air separation unit (ASU) and compression purification unit (CPU). For a  
43 conventional air-fired coal power plant, the net efficiency reduced by more than 10% when it is  
44 converted to oxy-firing [3-5].

45 In the first generation oxy-fuel technology, the ASU and CPU run under pressure, while the  
46 boiler is run at atmospheric pressure. Thus, the pressure fluctuation associated with the ASU,  
47 boiler and CPU cause energy losses and a reduction of net efficiency. However, for second  
48 generation oxy-fuel technology, or pressurized oxy-fuel combustion (POFC) technology, the  
49 whole system runs under pressure, and hence the work losses due to the pressure fluctuations can  
50 be substantially reduced. Together with this feature, many other advantages can also be achieved  
51 by deploying POFC [6-8] including: (1) recovering latent heat from flue gas; (2) increasing the  
52 convective heat transfer for a given mean velocity; (3) reducing the boiler size and equipment  
53 costs; (4) avoiding air ingress, thus ensuring the production of high purity of CO<sub>2</sub> in the flue gas  
54 and a relatively low purification cost; and (5) reducing the cost of flue gas recirculation fan and

the CPU system.

To date, many studies have contributed to the optimization of the POFC systems. Hong et al. [9,10] analyzed the ISOTHERM<sup>®</sup> pressurized oxy-combustion system of ENEL [11], and found the maximum efficiency could be achieved in the vicinity of the 1.0MPa operating pressure. The net efficiency showed nearly 3% increment at 1.0MPa over atmospheric combustion. Gopan et al. [12,13] introduced a staged pressurized oxy-combustion (SPOC) system with fuel staging and low flue gas recycle rate. The simulation of thermal system showed the optimal pressure was around 1.6MPa and the SPOC process increased the net efficiency up to 6% over conventional atmospheric oxy-combustion.

However, on the other hand, there are few experimental studies on the POFC. The only reported work includes coal combustion on the pressurized thermo-gravimetric analyzer (PTGA) [14-16] and fluidized bed [3,17]. Wang et al. [14] conducted the coal combustion experiments on the PTGA and the results indicated the effects of pressure on coal ignition mode. With the increase of pressure, the heterogeneous ignition at atmospheric pressure converted to homogeneous ignition at low and medium pressures, and then converted back to heterogeneous ignition at high pressure. Lasek et al. [3,17] investigated the effect of pressure on pollutant emissions, using a laboratory scale fluidized bed with continuous-feeding and found that NO, N<sub>2</sub>O, SO<sub>2</sub> emission were reduced under higher pressures during oxy-combustion.

As the first step of coal combustion, pyrolysis has great impact on the subsequent reactions. The conversion of N and S in the pyrolysis stage has an important influence on NO<sub>x</sub>/SO<sub>x</sub> emission and the operation safety of CPU system [18,19]. CO<sub>2</sub> is a reactant in the char gasification reaction, as well as one of the final product of coal pyrolysis, so the existence of high partial pressures of CO<sub>2</sub> affects the yield of volatile and N/S conversion significantly. Li et al. [20-25] conducted a series of studies on the pyrolysis characteristics of the Victorian brown coal, mainly focused on the generation of NO<sub>x</sub> precursors with different operating parameters like atmosphere and reactor types. The experiments show that CO<sub>2</sub> atmosphere surrounding coal/char particles can greatly affect the formation of NH<sub>3</sub> and HCN through its influence on the availability of H-radicals

[24,25]. The  $\text{CO}_2$  atmosphere tends to reduce the formation of  $\text{NH}_3$  and  $\text{HCN}$  if the thermal cracking of char generates a significant amount of H-radicals. Many efforts have been made to investigate the effects of other operation parameters like fuel type, temperature and heating rate on the formation of  $\text{NO}_x$  precursor during coal pyrolysis under  $\text{CO}_2$  atmosphere, and findings suggest that the  $\text{CO}_2$ -C gasification rate and the opening of -CN bond greatly affect the formation of  $\text{NH}_3$  and  $\text{HCN}$  [26,27]. However, these studies are limited to atmospheric pressure and there are still few studies about the effects of pressure on N conversion during coal pyrolysis under pure  $\text{CO}_2$  atmosphere.

Previous studies [28-30] have also revealed that the sulfur-containing gas and residual sulfur content in char during  $\text{CO}_2$  pyrolysis is highly depends on the minerals and sulfur forms in raw coal. Experimental work shows the high  $\text{CO}_2$  concentrations may promote the  $\text{CO}_2$  reduction reaction of pyrite and generate more  $\text{Fe}_3\text{O}_4$ ,  $\text{CO}$  and  $\text{SO}_2$  [31]. The results of pyrolysis experiment of coal under  $\text{N}_2$  and  $\text{CO}_2$  atmosphere by Karaca [32] indicate that  $\text{CO}_2$  atmosphere has more effects on the organic sulfur removal at high temperatures. Carbonate in coal can promote the decomposition of organic sulfur, and inhibit the decomposition of pyrite, while the silicate seems to promote the conversion from easily removable organic sulfur compounds to thermal stable organic sulfur compounds. At the same time, the effect of pressure on sulfur conversion during pyrolysis has mostly focused on pressurized hydro-pyrolysis studies, which showed that the increase of hydrogen pressure enhanced the removal of sulfur from coal [33,34].

Currently, information on N/S conversion of coal during pressurized pyrolysis under  $\text{CO}_2$  atmosphere is still limited, and a more complete understanding of the pathway for fuel-N and fuel-S conversion is important for future work on POFC technology, and in particular for gaseous pollutant control and system optimization. This information will also help to build up a comprehensive model of the PFOC by providing detailed reaction mechanisms. In this study, experiments on a lab-scale pressurized fluidized-bed system have been done to help determine the influence of pressure on the N/S conversion into both gaseous and solid products.

## 2. Experimental

### 2.1 Fuel and bed material

Table 1 shows the ultimate and proximate analysis of the bituminous coal used in the experiment. The sulfur speciation in the raw coal was determined according to the Chinese standard method (GB/T 215-2003), and is shown in Table 2. The particle size of coal ranged from 0.45 to 0.60mm. Silica sand (particle size: 0.25 to 0.35mm, true density: 2600kg/m<sup>3</sup>) was used as bed material, giving a static bed height of 0.3m.

### 2.2 Apparatus and procedure

Experiments were conducted on a 20kW<sub>th</sub> lab-scale pressurized fluidized bed system, as shown in Fig. 1, which consists of a bubbling fluidized bed combustor, gas distribution, feeding system, temperature and pressure controlling system, flue gas cooling system, and the gas analyzers. The combustor was made of the stainless steel, with an inner diameter of 50mm and a height of 1300mm. The combustor was placed in a pressure vessel, which was designed to withstand a pressure of 2.0MPa at 200°C. The bottom of the windbox was open, permitting the pressurized gas flowing into the riser to pass through it. During the experiments, the gas went into the pressure vessel first, and was heated by the reactor wall and then flowed into the windbox. However, because of this design, the pressure vessel is not operated at high temperature (<100°C). The flue gas leaving the reactor was then cooled down to 200°C by the gas cooler before entering the sampling line. A regulating valve was used at the outlet of the cooler to control the reaction pressure in the riser. The gas sampling line was connected to the sampling port after the regulating valve. The sampling line was electrically heated to control the temperature to around 165°C, to avoid the gas condensation. A filter was used to remove fine particles larger than 0.1μm from the flue gas. The Fourier transform infrared spectroscopy (FTIR) analyzer (Antaris IGS, Thermo Fisher Scientific Inc, USA) was used to monitor the composition of flue gas. The measuring accuracy of HCN/NH<sub>3</sub>/SO<sub>2</sub> was 0.01ppm.

The coal pyrolysis characteristics under N<sub>2</sub> and CO<sub>2</sub> atmosphere were investigated with the operation pressure ranging from 0.1 to 0.7MPa. The bed temperature in the dense zone was

controlled at 750°C, 800°C, 850°C and 900°C, respectively. Batch feeding was used in this experiment to avoid the unstable coal feeding under high pressure operation. Typically, 3-9g coal particles with the desired size were injected into the bottom zone of the reactor by the pressurized carrier gas. The gas velocity in the riser was normally in the range of 0.7-1m/s to guarantee the good fluidization of the silica sand bed material. Each test run was repeated 3-5 times to minimize the uncertainty in experiments.

### 2.3 Analysis methods of char

After each test, bed material was drained and char was removed by hand. This was easy to do since the colour of the coal char and sand are very different. The char produced at 850°C and CO<sub>2</sub> atmosphere was collected and analysed by a CTS5000B sulfur analyzer in order to obtain the sulfur content in the char. An X-ray photoelectron spectroscopy (XPS) analyzer (Escalab250Xi, Thermo Scientific Inc) was used to quantify the S form at the char surface. The XPS measurements in this study were carried out with an unmonochromated AlK $\alpha$  (1486.6eV) radiation. The step size was set as 0.1eV, and the internal standard calibration was set as C1s (284.6eV). The spectral features of S2p peak were used for sulfur speciation analysis.

In XPS analysis, the peak-fitting method is often chosen to identify the sulfur forms. The reliability of the peak data is highly dependent on the specific method and parameter setting of peak-fitting, and the two most common methods are  $2p_{3/2}/2p_{1/2}$  doublet fitting and  $2p_{3/2}$  single peak fitting.

Based on previous studies [35-37] and the XPS database of American National Institute of Standards and Technology (NIST) [38], the S2p<sub>3/2</sub> binding energies are summarized in Table 3. Each sulfur specie in Table 3 refers to a class of chemicals except pyrite. The binding energy of pyrite and sulfide have overlapping parts. Pyrite is the main sulfide components in coal, followed by marcasite, sphalerite and galena. In this paper, S content in coal is divided into five categories: sulfide/pyrite, thiophene, sulfoxide, sulfone and sulfate. The S2p<sub>3/2</sub> peak of sulfide is classified as pyrite. The XPS peakfit 4.1 software was used in the peak analysis and parameters setting is mainly based on the following principles [39]: (i) a 2:1 relative area was separated by 1.18 eV; (ii)

the L-G% (Lorentzian–Gaussian%) was set as 0; and (iii) the full width at half-maximum (FWHM) was set to the same value for each peak ranging from 0 to 2.

### 3. Results and Discussion

#### 3.1 Fuel-nitrogen releasing during pyrolysis

Pyridines, pyrrole, and quaternary nitrogen are the three principal N-compounds in the coal. Previous study shows that part of the pyridines and pyrrole nitrogen are converted to HCN during pyrolysis process [40]. The formation of  $\text{NH}_3$  has two main sources: one is the decomposition of quaternary nitrogen, while the other is the secondary reaction of tar and char. Fig. 2 presents the concentration of nitrogen-containing gases during coal pyrolysis under  $\text{N}_2$  and  $\text{CO}_2$  atmosphere at 0.5MPa and 850°C.  $\text{NH}_3$  and HCN are the major nitrogen-containing gases during coal pyrolysis, while NO and  $\text{N}_2\text{O}$  can also be detected in the gases produced. Because of the very low concentration of NO and  $\text{N}_2\text{O}$ , their curves are not included in Fig. 2. The  $\text{NH}_3/\text{HCN}$  ratios under both atmospheres are relatively low in this study, a result which is very different with that previously reported [24]. This difference may be caused by the differences in quaternary nitrogen content in various coals. Also from Fig. 2, the HCN concentration in  $\text{CO}_2$  atmosphere is higher than that in  $\text{N}_2$  atmosphere, owing to strong C/ $\text{CO}_2$  reaction in  $\text{CO}_2$  atmosphere. The gasification process breaks the stable –CN bonds and make it much easier to form HCN.

The HCN release profiles in different temperature at 0.5MPa and  $\text{CO}_2$  atmosphere are shown in Fig. 3. The peak value of HCN concentration curve increases as the pyrolysis temperature increases. As mentioned above, most of the HCN originates from the thermal-stable pyridines and pyrrole nitrogen in coal, and the higher temperature will increase their decomposition and generate more HCN [41]. In terms of nitrogen conversion, the nitrogen converted to HCN in  $\text{CO}_2$  and  $\text{N}_2$  atmosphere is 5.45 and 3.01 times of that converted into  $\text{NH}_3$  in  $\text{N}_2$  atmosphere. The existence of  $\text{CO}_2$  during pyrolysis clearly enhances total nitrogen conversion rate of coal. In Fig. 3, the higher pyrolysis temperature leads to a shorter time for HCN concentration to reach its peak value. This also can be explained by the thermal-stability of pyridines and pyrrole nitrogen.

Fig. 4 and Fig. 5 show the N-containing gases release profiles of coal at different pressure

189 and atmospheres. For the  $\text{NH}_3$  obtained in both atmospheres, with the increase of pressure the  
190 peak value of  $\text{NH}_3$  concentration shows a slight increase. The quaternary nitrogen is completely  
191 decomposed over  $800^\circ\text{C}$  [40]. Therefore, the influence of the pressure on the quaternary nitrogen  
192 decomposition at  $850^\circ\text{C}$  should be negligible. In addition, the direct hydrogenation of char-N by  
193 H-radicals is another important source of  $\text{NH}_3$  in the volatiles [22]. Higher pressure would slow  
194 down the diffusion of volatile precursors out from inside the particle, leading to increases in the  
195 residence time of volatile precursors inside the particles. This in turn intensify the thermal  
196 cracking of volatile precursors to produce more radicals, including H-radicals, and allow more  
197 time for the H-radical-laden volatile precursors to interact with the char-N to form  $\text{NH}_3$ .

198 From 0.1MPa to 0.7MPa the peak value of HCN concentration in  $\text{N}_2$  and  $\text{CO}_2$  atmosphere  
199 experienced a gradual rise. Pyridines and pyrrole nitrogen have a high thermal-stability, and are  
200 difficult to completely decompose even at  $1000^\circ\text{C}$ . However, high pressure is advantageous in  
201 enhancing the degree of pyrolysis, and the strong  $\text{C}/\text{CO}_2$  reaction in pressurized  $\text{CO}_2$  atmosphere  
202 breaks the stable -CN bonds of coal. And the exposed -CN sites encourage the formation of HCN  
203 with H-radical. It can be concluded that higher pressures enhance the generation of  $\text{NO}_x$   
204 precursors.

205 Fig. 6 presents the conversion rate under different temperature and pressure. Raising the  
206 temperature at each operating pressure will lead an incense to fuel-N conversion rate. At 0.1MPa,  
207 the nitrogen conversion rate from  $750^\circ\text{C}$  to  $900^\circ\text{C}$  increased by 4.49%. While at 0.7MPa, this  
208 increase is about 12.78%. Thus it is clear that increasing temperature and pressure jointly promote  
209 the conversion of fuel-N to  $\text{NO}_x$  precursors.

### 210 3.2 Sulfur conversion during pressurized pyrolysis

211  $\text{H}_2\text{S}$  and  $\text{COS}$  were not monitored in this study, however the sulfur content and sulfur  
212 speciation in the char residue were carefully investigated to provide us with additional information  
213 to better understand the sulfur chemistry under these conditions. During coal pyrolysis under  $\text{CO}_2$   
214 atmosphere,  $\text{SO}_2$  concentration in the gaseous product was monitored and the curves of  $\text{SO}_2$  under  
215 different pressure are shown in Fig. 7.  $\text{SO}_2$  concentration in the gaseous product is relatively low,



however as the pressure increases, this concentration has a slight decrease. Another interesting result is that the elevation of pyrolysis pressure leads to a reduction in the amount of sulfur in the char. The sulfur content in the char residue at 850°C is shown in Table 4. As the pressure increases, the sulfur content in char decrease, indicating that more tar-S and volatile-S are generated. As SO<sub>2</sub> also decrease with pressure, there may be more COS or H<sub>2</sub>S formation. By elevating the pyrolysis pressure, the high partial pressure of CO<sub>2</sub> enhances the formation of CO, which can be seen from Fig. 8. CO also appears to enhance the decomposition of sulfur in coal. This causes the drop of sulfur in char and creates more S-containing gases like H<sub>2</sub>S and COS. The high concentration of CO also enhances the conversion reaction from SO<sub>2</sub> to COS [28], as R1 and R2 show:



However, this is only one possible route for the simultaneous reduction of SO<sub>2</sub> and char residue sulfur as the pressure increases, and more experiments with accurate measurement of H<sub>2</sub>S and COS must be made to verify this explanation.

Fig. 9 shows the S2p<sub>3/2</sub> and S2p<sub>1/2</sub> doublet fitting results of raw coal and char obtained from pyrolysis under different pressures. In XPS peak fitting, the percentage of each peak area in relation to the total area is equated to the relative content of each sulfur form. Thus, based on the curve fitting results in Fig. 9, the distribution proportion of different sulfur forms is summarized in Table 5. The main sulfur forms in the raw coal surface is the sulfone (~37.32%) and thiophene (~23.29%), while the sulfide/FeS<sub>2</sub> only accounts for 16.04% of the total sulfur content of raw coal.

Sulfur conversion during coal pyrolysis is very complex. Sulfur-containing functional groups in coal decompose and release during pyrolysis process, and at the same time the interactions between pyrite, sulfate and organic sulfur also affect the distribution and speciation of sulfur in the final products. Zhang et al. [42] proposed a schematic of the sulfur conversion mechanisms during coal pyrolysis, as shown in Fig. 10, to illustrate the complex series of reactions.

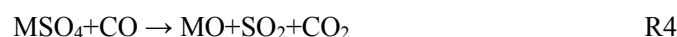
For coal pyrolysis under high pressure CO<sub>2</sub> atmosphere, the reaction mechanism in Fig. 10

still applies. However, with different pressure, the rate and extent of each reaction will be different. Thus, for instance, the increase of pressure causes the pyrite content to generally decrease. In reductive atmosphere, the decomposition reaction of  $\text{FeS}_2$  is mainly controlled by the following reaction:



The R3 reaction is one of the main sources of COS during coal pyrolysis. This reaction is very slow at  $800^\circ\text{C}$  [28]. Given the pyrolysis temperature and short residence time of coal in the fluidized bed, part of  $\text{FeS}_2$  will be converted to FeS, and will resist further reaction. The elevation of pressure enhances the reductive atmosphere through producing more CO, and accelerates the consumption rate of pyrite, so the pyrite content decreases when pressure increases.

The main kinds of sulfate in coal are the mixtures of  $\text{BaSO}_4$ ,  $\text{CaSO}_4 \cdot 2\text{H}_2\text{O}$ ,  $\text{CaSO}_4$  and  $\text{FeSO}_4$ , and these sulfates in the raw coal are typically only present at about 0.31% as shown in Table 2. Fig. 9 and Table 5 show the change of sulfate content is not obvious under different pressure. Two facts can be deduced about the influence of pressure on sulfate. One is that as the pressure increases, the sulfur fixation ability of the coal ash is likely to be enhanced [43], given that calcium, potassium and sodium in the ash can capture the  $\text{SO}_2$  in the gas more efficiently. The other is that as the pressure increase, higher concentration of CO will react with the sulfate to form  $\text{SO}_2$ , as show below:



Here M represents an alkali or alkaline earth metal. In addition, the reaction rate increases as the CO partial pressure increase. However, given that  $\text{SO}_2$  levels were not shown to be high in this study, we believe the first explanation is likely to be the more important one, and indeed we can see the overall sulfate content under high pressure is higher than that in low pressure.

Thiophene, sulfoxide and sulfone are usually referred to as organic sulfur in coal. The composition and structure of organic sulfur are very complex and with the total different thermal stability. Thiophene is much more stable and difficult to decompose because sulfur in the thiophene is aromatically bound [28]. The thiophene in coal can be generated from the two

reactions as shown in Fig. 10, one is S or H<sub>2</sub>S react with the organic matter in coal; The other is the pyrite reacts with small organic molecules like ethylene. When pyrolysis pressure increases, the relative content of thiophene will also rise. High pressure CO<sub>2</sub> promotes the gasification of coal and increases the concentration of small organic molecules, thus accelerating the generation of thiophene. Moreover, the decomposition of pyrite and sulfone reduces the total amount of sulfur in char under high pressure, so the relative content of thiophene which is thermal stable will increase.

Compared with the S<sub>2</sub> curves, the specific components of S<sub>3</sub> and S<sub>4</sub> curves are much more complex and difficult to specify. The thermal stability of sulfoxide and sulfone is highly dependent on the functional groups contacted with -SO<sub>2</sub>- and -SO-. Previous study [44] shows the thermal stability of sulfoxide and sulfone as follows: aliphatic sulfoxide < aromatic sulfoxide < sulfone < 650°C. So sulfoxide and sulfone decompose at experimental condition (850°C). The pyrolysis of coal makes the conversion of sulfoxide and sulfone into gaseous products, and the removal rate of them increase with the increase of pressure and the degree of gasification.

In summary, the possible pathway of how the high pressure CO<sub>2</sub> atmosphere affects sulfur conversion during pyrolysis appear to be as follows: (1) high pressure increases the sulfur conversion rate, resulting in more gaseous products like COS; (2) high partial pressure of CO accelerates the decomposition of pyrite; (3) the sulfur fixation ability of the ash is further enhanced by high pressure; (4) high pressure increases the conversion from gaseous S and pyrite to thiophene.

#### 4. Conclusion

Experiments on pyrolysis of coal at CO<sub>2</sub> atmospheres were conducted in a lab-scale pressurized fluidized bed system, and the influence of pressure on N and S conversion was explored. Some general conclusions can be drawn as follow:

- 1) For the raw coal in this experiment, HCN is the major nitrogen-containing gaseous product for coal pyrolysis at CO<sub>2</sub> atmosphere.

2) The generation of HCN and NH<sub>3</sub> increase simultaneously with the increase of overall pressure. High pressure and the existence of high partial pressures of CO<sub>2</sub> enhance the fuel-N conversion rate in pyrolysis process.

3) SO<sub>2</sub> concentration in gaseous product and sulfur content in char decrease simultaneously with the increase of overall pressure, indicating that more COS and H<sub>2</sub>S are generated during the pyrolysis process.

4) The effects of high pressure CO<sub>2</sub> on the migration of sulfur during pyrolysis are mainly due to the changes of volatile yield and the rate of sulfur conversion reactions. High pressure of CO<sub>2</sub> accelerates the decomposition of pyrite and also intensifies the conversion from gaseous S and pyrite to thiophene.

**Acknowledgements:** This work was financially supported by the National Natural Science Foundation of China (No.51206023).

#### **References**

- [1] Carbon Capture and Storage: The solution for deep emissions reductions, IEA, 2015.
- [2] Chen L, Yong S Z, Ghoniem A F. Oxy-fuel combustion of pulverized coal: Characterization, fundamentals, stabilization and CFD modeling[J]. Progress in Energy and Combustion Science, 2012,38(2):156-214.
- [3] Lasek J A, Janusz M, Zuwała J, et al. Oxy-fuel combustion of selected solid fuels under atmospheric and elevated pressures[J]. Energy, 2013,62:105-112.
- [4] Escudero A I, Espatolero S, Romeo L M, et al. Minimization of CO<sub>2</sub> capture energy penalty in second generation oxy-fuel power plants[J]. Applied Thermal Engineering, 2016,103:274-281.
- [5] Darde A, Prabhakar R, Tranier J, et al. Air separation and flue gas compression and purification units for oxy-coal combustion systems[J]. Energy Procedia, 2009,1(1):527-534.
- [6] Xia F, Yang Z, Adeosun A, et al. Pressurized oxy-combustion with low flue gas recycle:

317 Computational fluid dynamic simulations of radiant boilers[J]. Fuel, 2016.

318 [7] Zebian H, Mitsos A. Pressurized OCC (oxy-coal combustion) process ideally flexible to the  
319 thermal load[J]. Energy, 2014,73:416-429.

320 [8] Zebian H, Gazzino M, Mitsos A. Multi-variable optimization of pressurized oxy-coal  
321 combustion[J]. Energy, 2012,38(1):37-57.

322 [9] Hong J, Chaudhry G, Brisson J G, et al. Analysis of oxy-fuel combustion power cycle  
323 utilizing a pressurized coal combustor[J]. Energy, 2009, 34(9): 1332-1340.

324 [10] Hong J, Field R, Gazzino M, et al. Operating pressure dependence of the pressurized oxy-fuel  
325 combustion power cycle[J]. Energy, 2010, 35(12): 5391-5399.

326 [11] Gazzino M, Benelli G. Pressurised oxy-coal combustion Rankine-cycle for future zero  
327 emission power plants: process design and energy analysis[C]//ASME 2008 2nd International  
328 Conference on Energy Sustainability collocated with the Heat Transfer, Fluids Engineering,  
329 and 3rd Energy Nanotechnology Conferences. American Society of Mechanical Engineers,  
330 2008: 269-278.

331 [12] Gopan A, Kumfer B M, Phillips J, et al. Process design and performance analysis of a Staged,  
332 Pressurized Oxy-Combustion (SPOC) power plant for carbon capture[J]. Applied Energy,  
333 2014, 125: 179-188.

334 [13] Gopan A, Kumfer B M, Axelbaum R L. Effect of operating pressure and fuel moisture on net  
335 plant efficiency of a staged, pressurized oxy-combustion power plant[J]. International Journal  
336 of Greenhouse Gas Control, 2015, 39: 390-396.

337 [14] Wang C, Lei M, Yan W, et al. Combustion characteristics and ash formation of pulverized  
338 coal under pressurized oxy-fuel conditions[J]. Energy & Fuels, 2011, 25(10): 4333-4344.

339 [15] Lei M, Huang X, Wang C, et al. Investigation on SO<sub>2</sub>, NO and NO<sub>2</sub> release characteristics of  
340 Datong bituminous coal during pressurized oxy-fuel combustion [J]. Journal of Thermal  
341 Analysis and Calorimetry, 2016. doi:10.1007/s10973-016-5652-y

- 342 [16] Ying Z, Zheng X, Cui G. Pressurized oxy-fuel combustion performance of pulverized coal  
343 for CO<sub>2</sub> capture[J]. Applied Thermal Engineering, 2016, 99: 411-418.
- 344 [17] Lasek J A, Głód K, Janusz M, et al. Pressurized oxy-fuel combustion: A Study of selected  
345 parameters[J]. Energy & Fuels, 2012, 26(11): 6492-6500.
- 346 [18] Pipitone G, Bolland O. Power generation with CO<sub>2</sub> capture: technology for CO<sub>2</sub>  
347 purification[J]. International journal of greenhouse gas control, 2009, 3(5): 528-534.
- 348 [19] Kim S, Ahn H, Choi S, et al. Impurity effects on the oxy-coal combustion power generation  
349 system[J]. International Journal of Greenhouse Gas Control, 2012, 11: 262-270.
- 350 [20] Xie Z, Feng J, Zhao W, et al. Formation of NO<sub>x</sub> and SO<sub>x</sub> precursors during the pyrolysis of  
351 coal and biomass. Part IV. Pyrolysis of a set of Australian and Chinese coals[J]. Fuel,  
352 2001,80(15):2131-2138.
- 353 [21] Tan L L, Li C. Formation of NO<sub>x</sub> and SO<sub>x</sub> precursors during the pyrolysis of coal and  
354 biomass. Part II. Effects of experimental conditions on the yields of NO<sub>x</sub> and SO<sub>x</sub> precursors  
355 from the pyrolysis of a Victorian brown coal[J]. Fuel, 2000,79(15):1891-1897.
- 356 [22] Li C, Tan L L. Formation of NO<sub>x</sub> and SO<sub>x</sub> precursors during the pyrolysis of coal and  
357 biomass. Part III. Further discussion on the formation of HCN and NH<sub>3</sub> during pyrolysis[J].  
358 Fuel, 2000,79(15):1899-1906.
- 359 [23] Tan L L, Li C. Formation of NO<sub>x</sub> and SO<sub>x</sub> precursors during the pyrolysis of coal and  
360 biomass. Part I. Effects of reactor configuration on the determined yields of HCN and NH<sub>3</sub>  
361 during pyrolysis[J]. Fuel, 2000,79(15):1883-1889.
- 362 [24] Jamil K, Hayashi J, Li C. Pyrolysis of a Victorian brown coal and gasification of nascent char  
363 in CO<sub>2</sub> atmosphere in a wire-mesh reactor[J]. Fuel, 2004,83(7-8):833-843.
- 364 [25] Chang L, Xie Z, Xie K, et al. Formation of NO<sub>x</sub> precursors during the pyrolysis of coal and  
365 biomass. Part VI. Effects of gas atmosphere on the formation of NH<sub>3</sub> and HCN[J]. Fuel,  
366 2003,82(10):1159-1166.

- 367 [26] Li X, Zhang S, Yang W, et al. Evolution of NO<sub>x</sub> precursors during rapid pyrolysis of coals in  
368 CO<sub>2</sub> atmosphere[J]. Energy & Fuels, 2015,29(11):7474-7482.
- 369 [27] Duan L, Zhao C, Zhou W, et al. Investigation on coal pyrolysis in CO<sub>2</sub> atmosphere[J].  
370 Energy & Fuels, 2009, 23(7): 3826-3830.
- 371 [28] Attar A. Chemistry, thermodynamics and kinetics of reactions of sulphur in coal-gas  
372 reactions: A review[J]. Fuel, 1978, 57(4): 201-212.
- 373 [29] Wang P, Jin L, Liu J, et al. Analysis of coal tar derived from pyrolysis at different  
374 atmospheres[J]. Fuel, 2013,104:14-21.
- 375 [30] Hu H, Zhou Q, Zhu S, et al. Product distribution and sulfur behavior in coal pyrolysis[J].  
376 Fuel Processing Technology, 2004,85(8-10):849-861.
- 377 [31] Huang F, Zhang L, Yi B, et al. Transformation pathway of excluded mineral pyrite  
378 decomposition in CO<sub>2</sub> atmosphere[J]. Fuel Processing Technology, 2015,138:814-824.
- 379 [32] Karaca S. Desulfurization of a Turkish lignite at various gas atmospheres by pyrolysis. Effect  
380 of mineral matter[J]. Fuel, 2003,82(12):1509-1516.
- 381 [33] Chen H, Li B, Zhang B. Decomposition of pyrite and the interaction of pyrite with coal  
382 organic matrix in pyrolysis and hydropyrolysis[J]. Fuel, 2000, 79(13): 1627-1631.
- 383 [34] Xu W C, Kumagai M. Sulfur transformation during rapid hydropyrolysis of coal under high  
384 pressure by using a continuous free fall pyrolyzer[J]. Fuel, 2003, 82(3): 245-254.
- 385 [35] Grzybek T, Pietrzak R, Wachowska H. X-ray photoelectron spectroscopy study of oxidized  
386 coals with different sulphur content[J]. Fuel processing technology, 2002, 77: 1-7.
- 387 [36] Kozłowski M. XPS study of reductively and non-reductively modified coals[J]. Fuel, 2004,  
388 83(3): 259-265.
- 389 [37] Marinov S P, Tyuliev G, Stefanova M, et al. Low rank coals sulphur functionality study by  
390 AP-TPR/TPO coupled with MS and potentiometric detection and by XPS[J]. Fuel processing  
391 technology, 2004, 85(4): 267-277.

- 392 [38] <http://srdata.nist.gov/xps/selEnergyType.aspx>
- 393 [39] Wang Z, Li Q, Lin Z, et al. Transformation of nitrogen and sulphur impurities during  
394 hydrothermal upgrading of low quality coals[J]. Fuel, 2016,164:254-261.
- 395 [40] Duan L, Zhao C, Ren Q, et al. NO<sub>x</sub> precursors evolution during coal heating process in CO<sub>2</sub>  
396 atmosphere[J]. Fuel, 2011,90(4):1668-1673.
- 397 [41] Glarborg P. Fuel nitrogen conversion in solid fuel fired systems[J]. Progress in Energy and  
398 Combustion Science, 2003,29(2):89-113.
- 399 [42] Zhang D, Yani S. Sulphur transformation during pyrolysis of an Australian lignite[J].  
400 Proceedings of the Combustion Institute, 2011, 33(2): 1747-1753.
- 401 [43] Zakkay V, Clisset H, Ganesh A, et al. Sulfur retention of North Dakota (Beulah) lignite ash  
402 in PFBC[C]//ASME 1984 International Gas Turbine Conference and Exhibit. American  
403 Society of Mechanical Engineers, 1984: V003T05A014-V003T05A014.
- 404 [44] Van Aelst J, Yperman J, Franco D V, et al. Study of silica-immobilized sulfur model  
405 compounds as calibrants for the AP-TPR study of oxidized coal samples[J]. Energy & fuels,  
406 2000, 14(5): 1002-1008.



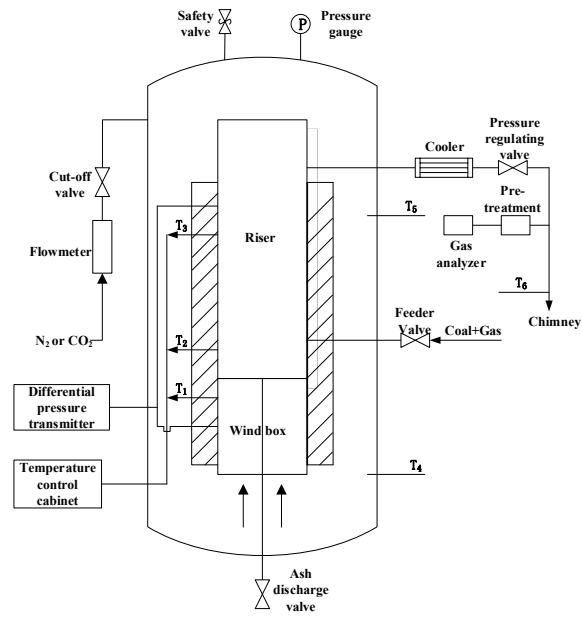


**Fig. 1.** Schematic diagram of pressurized fluidized bed system

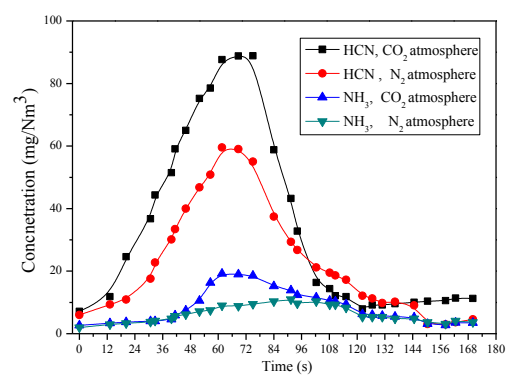


**Fig. 2.** Concentration of N-containing gases during coal pyrolysis at 0.5MPa and 850°C

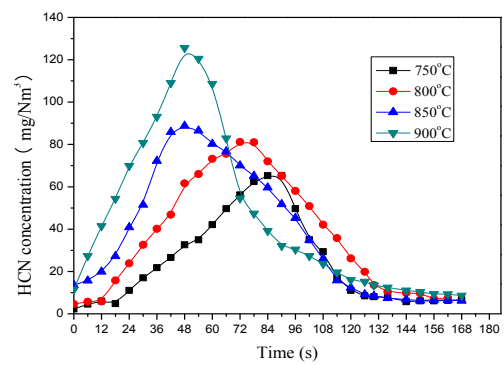


**Fig. 3.** HCN concentration curves of coal pyrolysis at 0.5MPa and CO<sub>2</sub> atmosphere

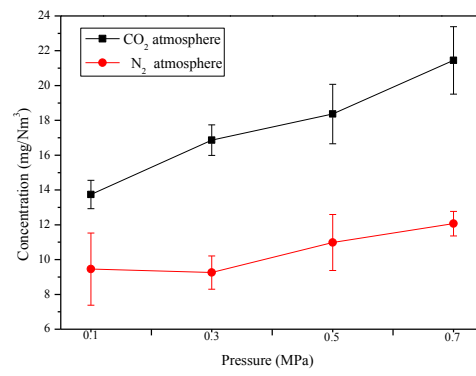
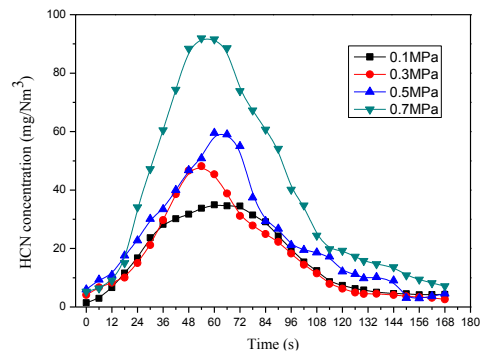
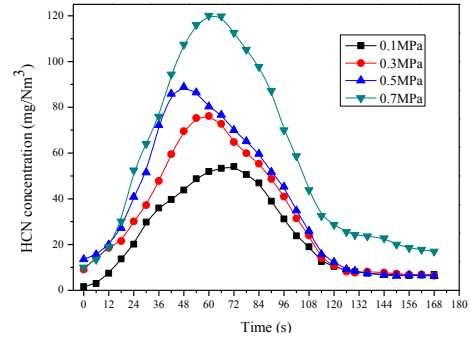


**Fig. 4.**  $\text{NH}_3$  peak concentration at  $850^\circ\text{C}$  with different pressure



(a) N<sub>2</sub> atmosphere



(b) CO<sub>2</sub> atmosphere

**Fig. 5.** HCN release curves of coal pyrolysis at 850°C with different pressure

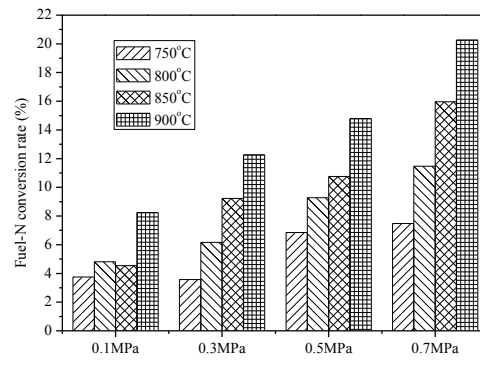


**Fig. 6.** Fuel-N conversion rate under CO<sub>2</sub> atmosphere at different temperature and pressure

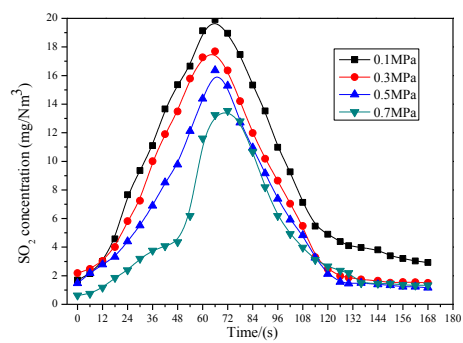


**Fig. 7.** SO<sub>2</sub> release curves of coal pyrolysis at 850°C and CO<sub>2</sub> atmosphere with different pressure

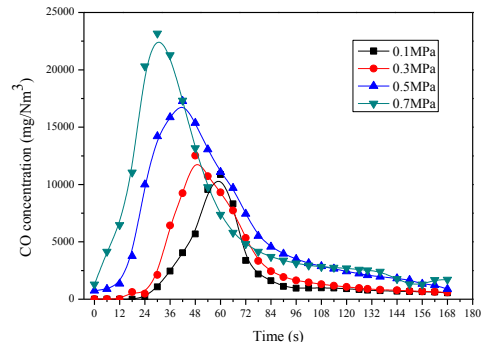
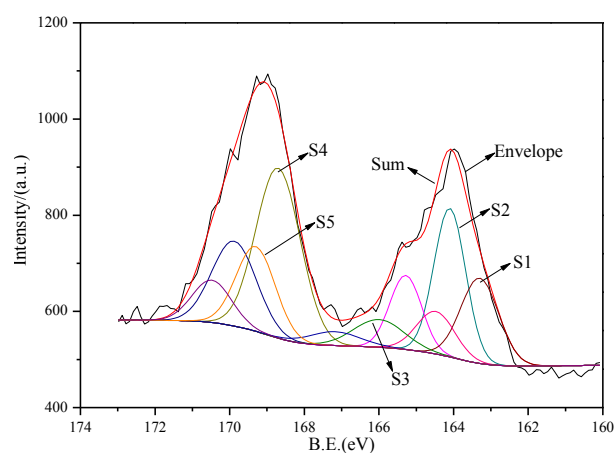
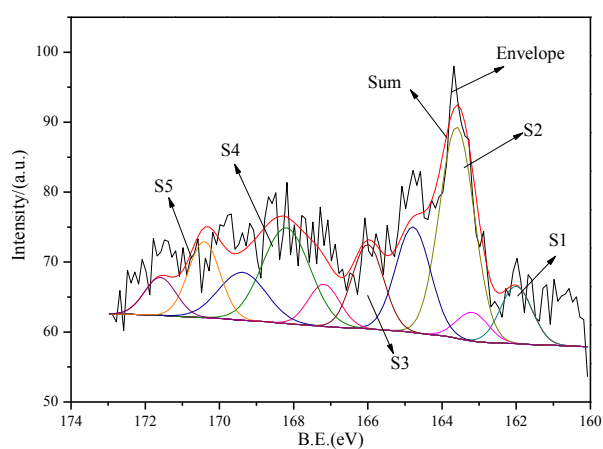


**Fig. 8.** CO release curves of coal pyrolysis at 850°C and CO<sub>2</sub> atmosphere with different pressure

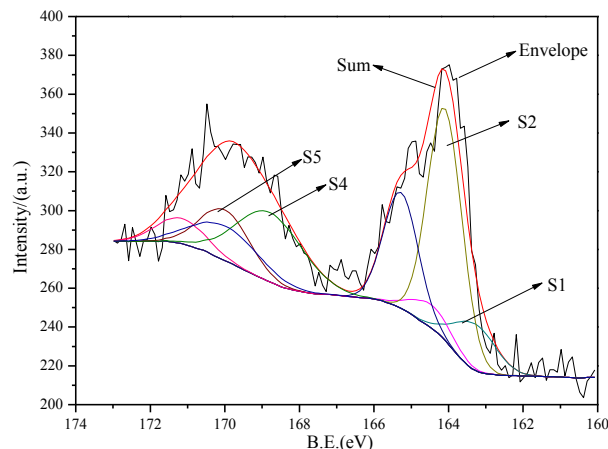




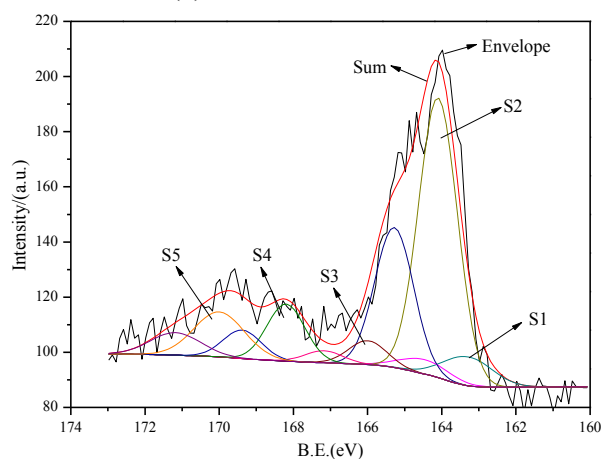
(a). Raw coal



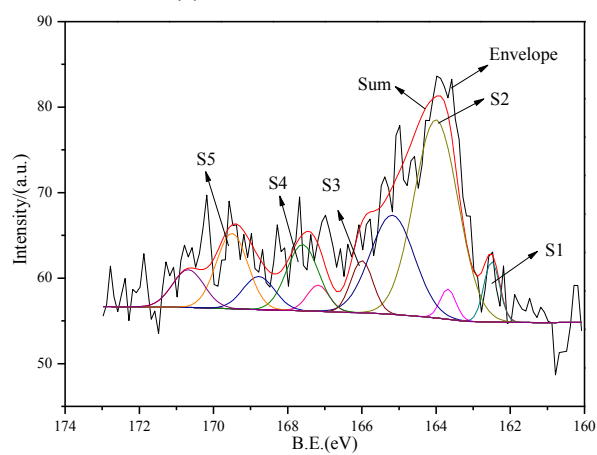
(b). Char under 0.1MPa



(c). Char under 0.3MPa



(d). Char under 0.5MPa



(e). Char under 0.7MPa

**Fig. 9.** Curve fitting results of raw coal and char

(S1-Pyrite peak; S2-Thiophene peak; S3-Sulfoxide peak; S4-Sulfone peak; S5-Sulfate peak)

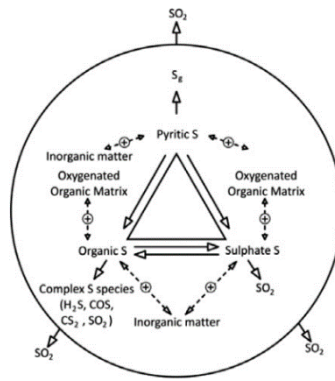


**Fig. 10.** A schematic of the mechanisms of sulfur conversion during coal pyrolysis [42]

**Table 1.** Ultimate and proximate analysis of raw coal / %

Coal samples	Ultimate analysis						Proximate analysis			Lower calorific value/ (MJ•kg <sup>-1</sup> )
	w(C <sub>ad</sub> )	w(H <sub>ad</sub> )	w(O <sub>ad</sub> )	w(N <sub>ad</sub> )	w(S <sub>ad</sub> )	w(M <sub>ad</sub> )	w(A <sub>ad</sub> )	w(V <sub>ad</sub> )	w(FC <sub>ad</sub> )	
Raw coal	67.42	4.14	8.31	1.04	2.72	6.52	9.85	35.34	48.29	26.66

\*ad denotes air dried basis

**Table 2.** Forms of sulfur in raw coal / %

Total sulfur	Pyrite sulfur	Sulfate sulfur	Organic sulfur
2.72	0.51	0.31	1.90

**Table 3.** Binding energies of S2p<sub>3/2</sub>

Sulfur species	Binding energy (eV)
Pyrite	162.3-162.9
Sulfide	162.1-163.6
Thiophene	164.0-164.4
Sulfoxide	165.0-166.0
Sulfone	167.0-168.3
Sulfate	> 168.4

**Table 4.** Sulfur content in char under various pressures

Pressure/MPa	0.1	0.3	0.5	0.7
w(Sulfur content)/%	2.37	1.93	1.75	1.64

**Table 5.** Distribution proportion of different sulfur forms after the curve fitting procedure

Sulfur species	Sulfur content w/%				
	Raw coal	Char under 0.1MPa	Char under 0.3MPa	Char under 0.5MPa	Char under 0.7MPa
Sulfide/Pyrite	16.04	12.20	11.14	8.07	6.36
Thiophene	23.29	38.13	46.98	62.26	58.10
Sulfoxide	6.93	9.68	0.00	5.18	8.11
Sulfone	37.32	28.17	27.25	11.46	11.55
Sulfate	16.42	11.82	14.63	13.03	15.88

# Nitrogen and sulfur conversion during pressurized pyrolysis under CO<sub>2</sub> atmosphere in fluidized bed

Duan, Yuanqiang

2016-10-25

Attribution-NonCommercial-NoDerivatives 4.0 International

---

Duan Y, Duan L, Anthony EJ, Zhao C. (2017) Nitrogen and sulfur conversion during pressurized pyrolysis under CO<sub>2</sub> atmosphere in fluidized bed. *Fuel*, Volume 189, February 2017, pp. 98-106  
<http://dx.doi.org/10.1016/j.fuel.2016.10.080>

*Downloaded from CERES Research Repository, Cranfield University*